Dead wood necromass in a moist tropical forest: Stocks, fluxes, and spatiotemporal variability

Evan M. Gora[1]*, Riley C. Kneale[1], Markku Larjavaara[2], and Helene C. Muller-Landau[3]

[1]Department of Biology, University of Louisville, Louisville, KY, USA

[2]Viikki Tropical Resources Institute (VITRI), Department of Forest Sciences, University of Helsinki, Finland

[3]Smithsonian Tropical Research Institute, Balboa, Ancon, Republic of Panama

*Author for correspondence: phone: 502-852-6771; email: evan.gora@louisville.edu

Abstract

Woody debris (WD) stocks and fluxes are important components of forest carbon budgets, and yet remain understudied, particularly in tropical forests. Here we present the most comprehensive assessment of WD stocks and fluxes yet conducted in a tropical forest, including one of the first tropical estimates of suspended WD. We rely on data collected over 8 years in an old-growth moist tropical forest in Panama to quantify spatiotemporal variability and estimate minimum sample sizes for different components. Downed WD constituted the majority of total WD mass (78%), standing WD contributed a substantial minority (21%), and suspended WD was the smallest component (1%). However, when considering sections of downed WD that are elevated above the soil, the majority of WD inputs and approximately 50% of WD stocks were disconnected from the forest floor. Branchfall and liana wood accounted for 17% and 2% of downed WD, respectively. Residence times averaged 1.9 years for standing coarse WD (CWD; >20 cm diameter) and 3.6 years for downed CWD. WD stocks and inputs were highly spatially variable, such that the sampling efforts necessary to estimate true values within 10% with 95%

Muotoiltu: Otsikko 1, Vasen, Riviväli: 1

Muotoiltu

confidence were >130 km of transects for downed CWD and >550 ha area for standing CWD. The vast majority of studies involve much lower sampling efforts, suggesting that considerably more data are required to precisely quantify tropical forest WD pools and fluxes. The demonstrated importance of elevated WD in our study indicates a need to understand how elevation above the ground alters decomposition rates and incorporate this understanding into models of forest carbon cycling.

Key words

carbon cycling, decomposition, snag, coarse woody debris, suspended woody debris, branchfall, Panama, liana

Manuscript Highlights

1. This is the most comprehensive description of dead wood cycling in a tropical forest
2. Half of dead wood is elevated above the ground, where decomposition is rarely studied
3. Sampling efforts needed to precisely quantify pools and fluxes are exceedingly large

Introduction

Tropical forests are currently the largest terrestrial carbon sink (Pan and others 2011) with most of their aboveground carbon stored in woody tissues. After wood dies, it serves a tremendous variety of ecological roles (reviewed by Harmon and others 1986) and constitutes ca. 10-20% of aboveground carbon storage and total CO_2 emissions in mature forests (Harmon and Sexton 1996; Brown 1997; Keller and others 2004; Palace and others 2007; Palace and others 2008; Malhi and others 2009; Anderson-Teixeira and others 2016). Although many aspects of woody debris (WD) cycling are well described (reviewed by Palace and others 2012), individual studies often focus on specific WD stocks or fluxes with low sampling efforts and without capturing their relative contributions. Consequently, the spatial and temporal distribution of WD remains poorly understood, particularly in understudied tropical forests (Palace and others 2012).

Woody debris is categorized by its size and location within a forest (Fig. 1). Traditionally, WD is separated into three pools defined by location: 1) *downed WD* that is in contact with the ground, 2) *standing WD* composed of standing dead trees (snags), and 3) *suspended WD* that is suspended in or attached to living trees or lianas (Swift and others 1976; Harmon and Sexton 1996). The majority of necromass is stored in large pieces of WD (coarse woody debris or CWD) and thus most studies either exclusively monitor CWD or separately record fine woody debris (FWD; Harmon and others 1986; Palace and others 2012). Downed WD is often greater than standing WD in mature forests, but the total amount of WD and its distribution among pools varies with stand age, forest structure, disturbance regime, management strategy and mean annual temperature (Janisch and Harmon 2002; Keller and others 2004; Eaton and Lawrence 2006; Sierra and others 2007; Kissing and Powers 2010; Palace and others 2012; Iwashita and others 2013; Gora and others 2014; Pfeifer and others 2015; Carlson and others 2017). The few comprehensive studies of suspended woody debris – primarily conducted in temperate forests – suggest that this pool can be comparable to or even greater than downed or standing WD pools

(Ovington and Madgwick 1959; Christensen 1977; but see Swift and others 1976). However, suspended WD is rarely quantified in tropical forests (Maass and others 2002) and, to our knowledge, never examined at large scales.

The categorization of WD into these three pools is based on methodological rather than functional differences, such as decomposition rate. Downed WD decomposes more rapidly than standing and suspended WD (Fasth and others 2011; Song and others 2017), whereas it is likely that standing and suspended WD decompose similarly (Swift and others 1976). Even among pieces of downed WD, those that are mostly elevated above the soil decompose ca. 40% slower than those with more soil contact (Přívětivý and others 2016). The elevated sections of downed WD pieces (i.e., sections that do not contact the ground; hereafter *elevated WD*; Fig. S1), experience different microclimate conditions, available nutrients, and fungal colonization patterns than sections of the same piece that contact the ground (Boddy and others 2009). These differences in abiotic conditions and decomposer community composition (Boddy 2001) are associated with different rates of decomposition (Boddy and others 1989; van der Wal and others 2015; Oberle and others 2017). Consequently, more functionally relevant categorizations of WD might differentiate pools based on whether a piece or section of WD directly contacts the forest floor.

As for the sources of WD, the relative contributions of different WD inputs reflect important aspects of forest carbon cycling. Each piece of downed WD is initially input from treefalls, branchfalls, or lianas, yet these distinct inputs are not typically distinguished from one another. Estimates of the proportion of inputs from branchfall are rare (Chave and others 2003; Palace and others 2008; Gurdak and others 2014; Marvin and Asner 2016), even though the proportion of tree biomass lost to branchfall is – or at least should be – an important parameter in carbon cycle models of forest vegetation (Clark and others 2001; Malhi and others 2011; Cleveland and others 2015; Doughty and others 2015; Marvin and Asner 2016). Branchfall is commonly omitted from tree mortality-based estimates of WD inputs (Chambers and others

2000; Meakem and others 2017), and these estimates inherently underestimate necromass production (Palace and others 2008). Lianas compose a small fraction of standing biomass (van der Heijden and others 2013), but their contributions to necromass pools and fluxes remain unknown. Lianas have relatively more vascular tissue and less recalcitrant structural tissue than similar diameter trees (Baas and others 2004) and thus liana wood is expected to decompose more rapidly than branch and trunk wood from trees (Harmon and others 1986). If liana abundance is increasing (Schnitzer and Bongers 2011), then the reduced size and persistence of liana WD relative to tree WD will magnify the effects of lianas in reducing forest carbon stocks (van der Heijden and others 2015).

Woody debris stocks and fluxes are highly variable in space and time, and quantifying patterns of WD aggregation and variation is necessary to understand WD dynamics and develop proper sampling procedures. In general, WD stocks and inputs are spatially aggregated at small scales (<50m, Woldendorp and others 2004) and highly variable in space and time, reflecting the rarity (and importance) of the large tree mortality and large branch mortality events that contribute the vast majority of WD (Palace and others 2008). Even within a single European forest, CWD volume differed by 8-fold (49 to 402 m^3 ha^{-1}) between nearby 1 ha plots characterized by similar management history and as being a single forest type (Král and others 2010). Similarly, CWD stocks and inputs because they differ by more than 20-fold (4.8-102.1 Mg ha^{-1}) even among undisturbed moist tropical forests (Palace and others 2012). Accordingly, accurate estimates of necromass require spatially and temporally extensive sampling to characterize the range of possible inputs and stocks, as well as their relative frequencies.

Here, we provide a comprehensive inventory of wood necromass in a lowland tropical forest, with a focus on poorly quantified aspects of woody debris stocks and fluxes and their spatiotemporal variation. We quantified not only the downed and standing pools, but also the suspended woody debris pool. We estimated the proportion of downed WD that is elevated and how this proportion changes during decomposition. We measured the proportion of downed

WD input from treefalls versus branchfalls, along with the relative contributions of branch, trunk, and liana wood. We calculated the sampling efforts necessary to estimate each stock and flux described here to within 10% of the true value with 95% confidence. Using a large-scale and long-term (2009-2016) dataset, we evaluated spatial and temporal patterns of CWD variation and aggregation. Finally, we estimated the residence time of downed and standing CWD using a steady-state model and by averaging measured decomposition rates of individual CWD pieces.

Methods

Study site

Field work was conducted in a mature, moist lowland tropical forest on Barro Colorado Island (BCI) in central Panama (9.152˚N, 79.847˚W; Hubbell and Foster 1983). The forest has an average annual temperature of 26˚C (2000-2017), mean annual rainfall of 2650mm (2000-2017), and a 4-month dry season (January-April, <100mm monthly rainfall; Paton 2017). Leigh (1999) provides a detailed description of this forest.

We estimated woody debris (WD) stocks, fluxes, and variability using line-intercept sampling for downed WD and area-based sampling for standing and suspended WD (Table 1; Rice and others 2004; Palace and others 2008). Most of our measurements were performed within a large 50 ha forest dynamics plot either along *long transects* spanning the length of the plot or in 100 40x40m subplots (the subplots are hereafter referred to as *dynamics plots* because they were used to track CWD dynamics; Fig. 2; Anderson-Teixiera and others 2015). Coarse and fine WD (i.e., WD with diameters >20cm or <20cm, respectively) were recorded separately in all cases. The minimum diameter for fine woody debris varied depending on the pool: for downed WD it was 2 cm where it crossed the transect, for standing WD it was 2 cm at 1.3 m height, and for suspended WD it was 5 cm at its largest end.

For simplicity, we describe the methodological approaches used in this study separately for each WD pool and measurement protocol in the following order: (1) we developed a photogrammetry technique to quantify suspended WD, (2) we quantified downed WD along the

long transects and along 40m transects in the dynamics plots, and (3) we monitored standing WD in the dynamics plots (Table 1). We also recorded the proportion of downed WD volume that does not directly contact the soil (referred to as *elevated WD*) along long transects in 2017 and 100m transects distributed across BCI in 2015. We report estimates of WD stocks and fluxes separately for each component and dataset (Table 1).

Photogrammetry of suspended and attached woody debris

We combined photogrammetry and methods typical of downed woody debris studies to estimate the volume of suspended woody debris in 10x10m subplots located in each corner of 50 dynamics plots (200 total subplots; Table 1, Fig. 2; see Supplementary methods). In addition to fully suspended WD, a minority of this pool exhibits minor contact with the forest floor, but was not typically included in our surveys of downed WD. Specifically, this WD was classified as suspended rather than downed if it did not contact the ground with at least three branches or a section of its main stem. We used Newton's formula to estimate the volume of suspended wood:

[1] $$V = l * \frac{(A_{e1}+4*A_m+A_{e2})}{6}$$

where V is volume (m^3), A is area (m^2) at each end ($_{e1}$, $_{e2}$) and at the midpoint ($_m$) of the woody debris, and l is the length of the woody debris (m, Harmon and Sexton 1996). We chose to use Newton's formula rather than other approaches (e.g., the frustum of a cone; Baker and others 2007) because it more precisely captures the irregular shape of decomposing WD (Harmon and Sexton 1996). We measured suspended WD if it was located in the crown or in resident lianas of any tree with more than half of its basal area inside the 10x10m subplot (Table 1, Fig. 2). To improve accuracy for irregular branches, we separately measured the diameters and length of each approximately linear subsection. For small terminal branches (N = 30) of these WD pieces, we measured their basal diameter and estimated their volume as cones ($\pi r^2 \frac{l}{3}$ where r is the basal radius (m) and l is the branch length (m)). In the small minority of cases in which the suspended woody debris was within reach of the ground, we took measurements by hand. In

other cases, we estimated dimensions using a combination of photographs and laser-based distance measurements (i.e., photogrammetry; Supplementary Methods; Wolf and Dewitt 2000). We confirmed the accuracy and precision of this approach in comparisons with direct measurements by hand (Supplementary Methods). We note that WD pieces within reach of the forest floor are sometimes recorded as downed WD (Pfeifer and others 2015); however, 79% of the suspended WD pieces measured in this study were not accessible from the ground and therefore would have been not included in other such studies.

We estimated branch length using angle and distance measurements. Using the same laser as above, we measured distance to both ends of the branch or branch subsection, and estimated the angle between the two measurements using a protractor and plumb line. We then calculated branch length using the Law of Cosines (Supplementary Methods).

Downed woody debris – Long transects

We used line-intercept sampling to quantify downed woody debris and distinguish its major components (Table 1, Fig. 2). To estimate total stocks, we measured FWD and CWD pieces that intersected long transects (500m) running North to South in the 50ha dynamics plot during 2010 and 2014, and both North to South (500m transects) and East to West (1km transects) during 2017 (Fig. 2). These transects were divided into 20m transect subsections, and FWD was recorded only in the first 1m of each subsection. For each piece of woody debris encountered, we recorded its diameter orthogonally to its longitudinal axis and centered around the intersection with the transect. To estimate wood mass, we performed destructive sampling of woody debris in 2010 to quantify wood density (as oven dry mass; g of dry mass per cm^3 of fresh volume) and described the relationship between real density and penetration with a dynamic penetrometer (See SI Methods). During 2010 and 2014, we estimated density in the field using a dynamic penetrometer (Larjavaara and Muller-Landau 2010) and in 2017 we estimated necromass using average density from the 2010 surveys (Table 1). In 2017, we categorized downed CWD along three dimensions: (1) elevated above the soil (i.e., *elevated WD*;

Fig. S1) or in direct contact with soil, (2) originating from a branchfall or treefall, and (3) constituting trunk wood, branch wood, or liana wood.

Downed woody debris – Dynamics plots

To quantify stocks, inputs, outputs, and spatiotemporal variability of downed CWD, we performed line-intercept sampling along the four 40-m transects within each of the 100 dynamics plot (Table 1; Fig. 2). These transects were surveyed from 2009 to 2016 (excluding 2011) and each piece of woody debris encountered was uniquely tagged and assigned a transect subsection (10m) identification number. Diameter and penetrometer-estimated density were recorded yearly for all pieces of CWD with diameters >20cm. We only estimated CWD inputs when CWD also was surveyed in the previous year (2010 and 2013-2016). In 2015 and 2016, we recorded whether new pieces of CWD were input via branchfall or treefall and whether the treefall inputs were composed of branch wood or trunk wood.

Downed woody debris – Estimates

We integrated over the cross-sectional area or mass encountered to obtain volume or mass, respectively, of woody debris per area of ground (Warren and Olsen 1964; Larjavaara and Muller-Landau 2011). For unidirectional transects (i.e., 2010 and 2014 long transects), we divided cross-sectional mass (or cross-sectional area) by the sine of the angle between the longitudinal axis of the piece of WD and the transect itself to account for the orientation of diameter measurements relative to the piece of CWD rather than the transect itself. For bidirectional transects (dynamics plots and 2017 long transects), we multiplied sample cross-sectional mass and cross-sectional area by the random angle correction factor ($\pi/2$). We then summed angle-corrected cross-sectional mass and cross-sectional area across all samples, and divided by total transect length.

Downed woody debris – Short transects

In addition to the 2017 long transects, we also quantified the proportion of downed WD elevated above the forest floor (i.e., *elevated WD*; Fig. S1) using 33 short transects in 2015

(100m; Table 1). These transects began every 200m along the trail system on BCI and ran orthogonally to the trails themselves, thus sampling the entire landscape of the island. By contrast, the 50ha forest dynamics plot is located in large part on a plateau and is unrepresentative of the larger landscape in its topography (Johnsson and Stallard 1989). This difference matters because the proportion of elevated WD is affected by local topography (Přívětivý and others 2016). We classified each piece of WD into one of five decomposition classes (Harmon and others 1995), measured its average cross-sectional area (i.e., volume over length), and evaluated the proportion of elevated WD across the entirety of each piece of WD encountered (Fig. S1). Volume of each subsection was measured using *equation 1*. We then took a weighted average of the elevated proportion of WD over pieces, weighting by average cross-sectional area, to estimate total elevated proportion of WD at the forest-scale. We tested for differences in the proportion of elevated wood per piece of downed woody debris among decomposition classes using ANOVA. When possible, we performed paired penetrometer measurements of adjacent WD subsections that were elevated or in direct contact with the forest floor (N = 78). We compared penetrometer penetration and estimated density of adjacent downed and elevated sections of downed CWD using paired t-tests.

Standing woody debris

We censused standing CWD in the entire area of the dynamics plots from 2009-2016 (excluding 2011). We estimated CWD stocks each year, and we estimated inputs when standing CWD also was surveyed in the previous year (2010 and 2013-2016). Standing CWD was defined as standing WD with a DBH (diameter at breast height, i.e., 1.3 m height) > 20 cm. We measured the height, penetration using dynamic penetrometer, and DBH of each tree. For buttressed trees, we estimated the equivalent diameter at 1.3 m height using a taper function (Cushman and others 2014). Previous work suggested the relationship between penetration and wood density was the same for standing and downed CWD (Larjavaara and Muller-Landau 2010), and thus we estimated density with the density-penetration relationship described with

destructive sampling in 2010. These individualized density estimates were used to calculate necromass.

We estimated volume differently for relatively intact and mostly decomposed snags. We qualitatively recorded whether standing CWD retained few (<10% of branches), some (10-90% of branches), or nearly all (>90%) of its branches. For standing CWD with some or all of its crown, we estimated necromass using an environment-specific biomass function (Chave and others 2014):

[2] $$AGB = e^{-1.803-0.976*E+0.976*\ln(\rho)+2.673*\ln(D)-0.0299[\ln(D)^2]}$$

Where AGB is aboveground biomass (kg), E is a region-specific environmental parameter (E = 0.0561 for BCI), D is DBH (m), and ρ is wood density (kg m^{-3}). We assumed that biomass equaled necromass for trees with intact crowns. For trees with part of their crown missing, we estimated that 50% of branches were lost and, because branch wood is ca. 25% of total biomass, we estimated necromass as 87.5% of original biomass (Falster and others 2015). For standing CWD that lacked branches, we used a taper function to estimate diameter at the top of the remaining trunk (Cushman and others 2014) and approximated volume as a truncated cone.

We quantified standing FWD in a 5m radius subplot (78.5m^2) centered within each dynamics plot (100 plots; Table 1). We recorded DBH and height for standing FWD, and estimated volume using the same truncated cone approach described above. To estimate stocks and fluxes, standing and suspended woody debris volume and mass were summed across all samples, and divided by total area.

Calculations of fluxes, stocks, and sampling efforts

CWD inputs and outputs were estimated from the yearly surveys of the dynamics plots. We estimated the mean residence time of CWD using a steady state model; we divided the mean stocks (7 years of estimates) by the mean inputs (5 years of estimates). We then estimated the decomposition constant, k, as 1 divided by the residence time. Using the decomposition constant, we then recalculated estimates of the inputs to account for the mass and volume lost

between when a sample entered the system and when it was first recorded, using the following equation based on instantaneous decomposition rates:

[3] $$V_{i,0} = V_{1,t}\frac{r}{1-e^{-rt}}$$

where $V_{i,0}$ and $V_{1,t}$ are the values (volume, mass, cross-sectional area, or cross-sectional mass) for sample i at the time it was input and the time it was recorded, respectively, t is time since the previous census (years – always "1" in our analyses), and r is the decomposition constant (years^{-1}; see SI for derivation). We then iteratively recalculated the total inputs and the decomposition constant until the change in r was less than 1% of its total value.

We also calculated alternative estimates of residence times using changes in the mass and cross-sectional mass of individual CWD pieces. For CWD pieces that still qualified as CWD in the subsequent census, we calculated absolute changes in their mass and volume and calculated the decomposition constant for each year using an exponential decay model (Supplementary methods). We averaged decomposition constants for pieces of CWD that were remeasured multiple times so that each piece of CWD was represented by a single decomposition constant. For CWD pieces that exited the CWD pool before the next census, we calculated minimum and maximum mass loss under several alternative assumptions about the remaining (unmeasured) mass and volume (Table S1). To account for differences in the size of CWD pieces, we weighted decomposition constants by the cross-sectional-mass and mass (rescaled from 0-1) of each piece of downed and standing CWD, respectively.

For all stocks, fluxes, and proportions, we calculated confidence intervals by bootstrapping over spatial subsamples – either transect sections (10 or 20 m in length) or subplots (100 m^2 each). When individual density estimates were not available, we estimated oven dry mass by multiplying final volume estimates by average dead wood density from the 2010 long transects (0.271 g cm^{-3}; See SI methods). We further calculated the sampling effort necessary to estimate pools and fluxes within 10% of the true value with 95% confidence given the observed variability. Specifically, we calculated the total transect length (km) or surveyed

area (ha) that would meet these criteria from the observed coefficient of variation (Metcalfe and others 2008; Supplementary methods).

Analyses of spatial and temporal autocorrelation

We tested for and quantified spatial autocorrelation in downed and standing CWD pools within and across our sampling units (transect sections and subplots, respectively). We generated separate omnidirectional semivariograms for mass, volume, and number of pieces of stocks and inputs of downed and standing CWD in the dynamics plots. We used each transect section (10-m) or quadrat (100 m^2) as a separate data point and ran separate analyses for each year (R package *GeoR*). Semivariograms were calculated using 10 m bins and extending to 250 m, half the minimum dimension of the 50 ha plot. Because the data were generally overdispersed and included many zeros, we log (x+1) transformed mass and volume before creating semivariograms. To test for aggregation within our sampling units, we fit Poisson and negative binomial distributions to the distributions of standing and downed CWD pieces across samples (R package *fitdistrplus*). We used maximum likelihood estimation and compared fits of the Poisson and negative binomial distributions using AIC values (Delignette-Muller and Dutang 2015). CWD counts per quadrat or transect section will follow a Poisson distribution if individual pieces are independently distributed, and a negative binomial distribution if pieces are non-randomly clumped together. For the negative binomial distribution, the overdispersion "size" parameter characterizes the degree of non-random aggregation; smaller values of this parameter indicate greater aggregation. Finally, to evaluate the potential for temporal autocorrelation in woody debris inputs, we tested if inputs were more likely in 10 m and 100 m^2 subsamples that received inputs the year before using Fisher's exact tests (*Binomial tests*).

All calculations and statistical analyses were performed in the R statistical environment (version 3.4, R Core Team 2017).

Results

Pools and inputs of woody debris

The majority of wood mass was in CWD (i.e., pieces with a diameter > 20 cm) and stored in the downed WD pool (Fig. 3). Total WD (20.63 Mg ha-1) was compromised of suspended woody debris (1.1%; 0.23 Mg ha^{-1}), standing WD (20.9%; 4.3 Mg ha^{-1}) and downed WD (78%; 16.1 Mg ha^{-1}; Fig. 3). Nearly all pieces of suspended wood were FWD (91%), and suspended FWD volume was nearly three times greater than that of suspended CWD. By contrast, downed CWD mass was approximately three times greater than downed FWD, and the mass of standing CWD stocks was nearly 4000 times greater than standing FWD (Fig. 3, Tables S2 and S3). Considering all pools of WD, the majority of dead wood mass was stored in pieces of CWD (77%, Fig. 3).

A large portion of downed WD > 10cm diameter is elevated above the forest floor (Fig. 4). The 2017 long transects found that 23% (CI: 14-34%) of downed WD stocks in the 50 ha plot were elevated above the forest floor, whereas the short transect surveys found 52% of downed WD stocks were elevated (N = 177, CI: 46-57%) in other areas of the island. The actual proportion of elevated WD likely falls between these two estimates because of opposing biases. Specifically, the short transects overestimate the frequency of longer pieces of WD that tend to be more elevated, whereas the long transects sampled an area that lacks diverse topography and experiences heavy foot traffic that collapses elevated WD (Gora, pers. obs.; see Supplementary Information for more details). The proportion of elevated WD decreased with increasing decay stage ($F_{4,172} = 14.51$, $p < 0.001$; Fig. 4), and the elevated sections decomposed more slowly. Penetrometer penetration was 250% deeper for downed sections of WD than for adjacent elevated sections of the same piece (15 vs. 6 mm per hit; $t = 2.52$, d.f. = 78, $p = 0.014$) suggesting that wood density was 11% higher in elevated WD (0.259 vs. 0.232 g cm^3; $t = 4.09$, d.f. = 78, $p < 0.001$). Combining elevated sections of downed WD with suspended and standing pools shows that approximately half of WD stocks are not in contact with the forest floor (43% if assuming only 23% of downed stocks are elevated; 65% if assuming 52% elevated). An even higher proportion of WD begins decomposing above the forest floor given that elevated, suspended,

and standing WD often transition to the downed WD pool. In the context of the standing and downed CWD inputs measured here (Fig. 3), this suggests that substantially more than 54% (or 71% if we assume 52% of WD is elevated) of total WD was input as elevated, standing or suspended WD.

Branchfalls were responsible for only a small minority of downed WD inputs and stocks, and branch wood accounted for a minor portion of treefall WD (Tables 2, S5-S6). Specifically, branchfalls accounted for 17% (CI: 11-26%) of total downed WD stocks but, because branchfalls are typically smaller pieces of WD, they were only 4% (3-6%) of downed CWD stocks and 10% (4-22%) of CWD inputs. Combining branch wood in treefalls with branchfalls, total branch wood accounted for 23% (CI: 14-36%) of downed WD stocks and ca. 21% of CWD inputs (Table 2). Liana wood also was input into the downed WD pool, but it only contributed 2% (CI: 2-4%) of total downed WD volume and liana wood was restricted almost entirely to FWD (12% of total FWD, CI: 6-21%). Overall, 6% of WD stocks and 23% of WD inputs could not be classified as branchfall or treefall.

Aggregation and spatiotemporal variability of CWD

WD stocks and inputs had high spatial variability. For CWD, which accounts for the large majority of stocks and inputs, the coefficient of variation across 10-m and 100-m^2 sampling units ranged from 601% to 1580%, meaning the standard deviation was 6 to 16 times greater than the mean (Table 3). This pattern was caused by rare, exceptionally large CWD pieces combined with a large majority of sampling units with no CWD (Figs. S4-5). Standing and downed CWD pieces were non-randomly distributed across sampling units, with the number of pieces encountered similarly or better fit by the negative binomial distribution than by the Poisson distribution in 13 of the 14 occasions that spatial aggregation was recorded (Table S7). However, we could not identify spatial structure in WD pools above the scale of our smallest sampling units (10-m and 100-m^2), as demonstrated by semivariogram analyses (Fig.

S5) and further confirmed by the predictable scaling of the coefficient of variation with increasing sampling scale (Table S8).

Because of this extreme spatial variability, substantial sampling efforts are necessary to precisely estimate WD stocks and fluxes. CWD and fluxes typically required larger sampling efforts than FWD and stocks because they were less frequent and the size range of FWD was more constrained (<20 cm, Table 3). By contrast, the size distribution of CWD was strongly right-skewed and thus a huge sampling effort was necessary to characterize the frequency of large, high-leverage inputs (Fig. S3-S4). Insufficient sampling efforts either overestimate or underestimate the frequency of large inputs, leading to chronic imprecision and misleading estimates. Small sampling efforts that miss large pieces of CWD will underestimate stocks and fluxes (e.g., CWD from the 2014 long transects; Fig. 5), whereas similar sampling efforts that encounter large pieces of WD will overestimate the stock or flux. The skewed distribution of WD sizes even inhibits predictions of the sampling efforts necessary for precise estimates. For example, the target sampling efforts that were estimated with less effort in this study tended to be smaller than those estimated with greater effort (Table 3).

Despite limited spatial structure, CWD inputs were non-randomly aggregated through time. Downed CWD inputs occurred 290%, 250%, and 180% more frequently than expected if a piece of CWD was input on the same 10-m transect section 1 year (Binomial test: $p < 0.001$), 2 years ($p < 0.001$), and 3 years prior ($p = 0.05$), respectively. There was no association with downed inputs 4 years prior (Binomial test: $p = 1.0$). This pattern is likely the result of gap expansion or fragmentation of a standing dead tree as it enters the downed CWD pool over multiple years. By contrast, standing CWD inputs were not associated with previous inputs at the 100 m^2 (Binomial test: $p = 0.098$) or 1600 m^2 sampling scales (Binomial test: $p = 0.975$). Note that we have low power to detect differences in stocks and fluxes among years. The calculated sample efforts necessary for precise estimation of CWD stocks and inputs were >130 km and > 500 ha, many times greater than the annual sample efforts in this study (16 km, Table

3). Consequently, our results should not be interpreted as evidence that CWD stocks and inputs are temporally homogenous; rather, qualitative comparisons of CWD stocks, fluxes, and patterns of aggregation suggest that inputs and stocks vary year-to-year (Figs. 4 and S2, Tables S2-S4).

Residence time and decomposition constants

The average residence times calculated from a steady state model were 1.8 (2.0) years for standing CWD mass (volume) and 3.4 (3.6) years for downed CWD. Correspondingly, this indicates that 2.3 Mg ha^{-1} and 3.5 Mg ha^{-1} of wood necromass are output from the standing and downed CWD pools, respectively. Residence times calculated from remeasurements of individual pieces were considerably more variable (Table 4, Table S1). This variability was likely due to large differences in decomposition rates among pieces of CWD and imprecision associated with individual measurements of CWD density and diameter. The steady state estimates closely resembled the individualized estimates assuming complete decomposition, suggesting that most of the pieces of CWD that fell below the minimum measurement threshold decomposed completely. Finally, sensitivity analysis revealed that individualized estimates were more sensitive to changes in diameter than changes in density (Table S1).

Discussion

Accurate estimates of WD pools and their spatiotemporal dynamics are necessary to understand carbon cycling. Here, we conducted the most comprehensive survey of WD in any tropical forest. Using the first-ever estimate of elevated WD in any forest type, we show that the majority of wood necromass is decomposing separated from the forest floor. We also demonstrate that uncommonly large sampling efforts are necessary to precisely estimate WD pools and fluxes due to the highly variable nature of CWD. These findings challenge the precision and reliability of many WD estimates and emphasize the need to consider the vertical distribution of WD *in situ*.

The contemporary understanding of decomposition processes is based on ground-level studies (Adair and others 2008; Bradford and others 2014), yet half or more of total WD stocks often are separated from the forest floor (more than 70% of total WD; Maass and others 2002). Although we encountered relatively little suspended WD in this study, substantially larger estimates in other forests indicate that suspended WD mass varies among sites (Ovington and Madgwick 1959; Swift and others 1976; Christensen 1977). Regardless, standing WD alone can exceed total downed WD in undisturbed tropical forests (Delaney and others 1998; reviewed by Palace and others 2012), and here we show that an additional 25-50% of downed WD is actually elevated. We suggest that functionally relevant categorizations of WD should delineate whether a piece or section of WD directly contacts the forest floor.

Decomposition rates differ substantially between the forest floor and standing, suspended, or elevated WD (Fasth and others 2011; Přívětivý and others 2016; Song and others 2017), but the relative contributions of differences in moisture content, nutrient availability, and organismal effects are untested in this context. Recent work has shown that decomposer communities and activities differ dramatically along a vertical gradient within tropical forests (Gora and others This Issue, Law and others This Issue). Termites readily consume ground-level WD while largely ignoring suspended wood (Law and others This Issue), and slower decomposition above the forest floor is associated with the decreased abundance of fungal decomposers and increased abundance of bacterial decomposers (Gora and others This Issue). However, our general understanding of how wood decomposes and how to model wood decomposition still relies on ground-level studies (Thornton 1998; Liski and others 2005; Weedon and others 2009; reviewed by Cornwell and others 2009; but see Mäkinen and others 2006) and/or experiments that only consider completely downed pieces of WD (i.e., no elevated WD; van Geffen and others 2010; Cornelissen and others 2012; Bradford and others 2014; Zanne and others 2015). Until decomposition is viewed as a holistic process that incorporates

aboveground decomposition, the factors that regulate wood decomposition and related aspects of carbon cycling will remain poorly understood.

Necessary sampling efforts will differ among sites depending on local spatiotemporal variation, but our results indicate that WD stocks and fluxes require large efforts for precise quantification. Without sufficient sampling efforts, studies will only fortuitously capture the true (or "real") frequency of large pieces of WD (Fig. S4). The problems caused by these unusually large inputs are known (Palace and others 2008), but even relatively large-scale studies typically lack sufficient sample sizes for precise quantification (Rice and others 2004; Palace and others 2008; Carlson and others 2017). Temporal variability, while undescribed, is likely substantial and further complicates the problem of quantifying WD stocks and fluxes. Because studies generally lack sufficient sampling efforts and many do not bootstrap over spatial sampling units, existing estimates of WD are generally imprecise and often underestimate their uncertainty (Chambers and others 2000; Palace and others 2008). Fluxes require larger sample sizes than stocks (Clark and others 2002), and larger sample sizes likely are also needed to precisely estimate residence times. For example, the much-cited highest measured CWD decomposition rate in tropical forests was based on data from only 1.5 ha and could be a statistical outlier rather than representative of the local forest (Delaney and others 1998; Palace and others 2012). The necessarily imprecise estimates of WD based on smaller datasets are useful starting points, but should be interpreted cautiously, particularly as parameters of global carbon cycling models.

Forest dynamics studies offer an alternative method for estimating WD fluxes using tree mortality and branchfall (Meakem and others 2017). Co-located with our study, Meakem and colleagues (2017) estimated WD (> 10cm DBH) inputs from tree mortality as 5.4 Mg ha^{-1} yr^{-1} from 1985-2010. Branchfall was not included in this mortality-based estimate, and we see that the difference between our estimate of WD inputs and Meakam's (9%) nearly equals the proportion of WD input as branchfall (8%, Table S5; also see Chave and others 2003). This

confirms that mortality-based estimates can be accurate for the treefall component of WD inputs. However, estimates of total branchfall range over 15-45% of all WD inputs (Malhi and others 2014; Marvin and Asner 2016) and the reasons for differences in branchfall are unclear. Consequently, tree mortality-based estimates of WD inputs require coordinated branchfall measurements to account for potentially large differences in branchfall inputs among sites.

Although direct comparisons with other forests are difficult, the WD stocks observed on BCI appeared relatively low (Baker and others 2007). Our estimates of residence times for standing CWD are shorter than the three previous estimates from tropical forests (Odum 1970; Lang and Knight 1979; Palace and others 2008) and downed CWD residence times were shorter than most tropical estimates (Palace and others 2012). Given the substantial mass of CWD inputs in our study, the fast rates of decomposition likely caused the relatively low WD stocks observed here. Although we did not test mechanisms of decomposition, previous work concluded that oceanic sodium deposition caused faster rates of wood decomposition on BCI than in an inland Ecuadorian forest (Kaspari and others 2009; Clay and others 2015). The possibility that regional abiotic conditions, such as proximity to salt water, can dramatically change decomposition rates emphasizes the need for replicated studies quantifying WD stocks and fluxes across a broad range of forests.

Recommendations and conclusions

This study provides a framework for the interpretation and design of forest inventory studies. Given the spatial variability observed here, future studies of WD should involve large sampling efforts to improve their precision, and all studies should use bootstrapping of spatial sampling units in estimating confidence intervals. The majority of variability in WD estimates was due to differences in wood volume, thus we suggest sacrificing estimates of wood mass for greater sampling of wood volume when resources are limited. As for quantifying spatial structure, area-based approaches are preferable to line intercept sampling as they do not miss pieces of WD. Additionally, by applying these recommendations across years, it will finally be

possible to explore temporal variation in WD stocks and fluxes. Without precise and reliable estimates of WD, global carbon models are difficult to parameterize and the exact contribution of WD to carbon cycling remains unclear (Pan and others 2011). Addressing these considerations in future studies should reduce uncertainty in forest inventories, thus improving our understanding of carbon cycling and related processes.

Acknowledgements

We thank Oris Acevedo, Melissa Cano, and the Smithsonian Tropical Research Institute for logistical support. We thank Pablo Ramos and Paulino Villarreal for field assistance. Comments from two anonymous reviewers improved the manuscript. This research was supported in part by the HSBC Climate partnership and the Smithsonian ForestGEO program through H.C. Muller-Landau, and a Smithsonian Tropical Research Institute Fellowship and NSF grant GRF-2015188266 to E.M. Gora.

References

Adair EC, Parton WJ, Del Grosso SJ, Silver WL, Harmon ME, Hall SA, Burke IC, Hart SC. 2008. Simple three-pool model accurately describes patterns of long-term litter decomposition in diverse climates. Global Change Biology 14: 2636-2660.

Anderson-Teixeira KJ, Davies SJ, Bennett AC, Gonzalez-Akre EB, Muller-Landau HC, Wright SJ, Salim KA, Zambrano AMA, Alonso A, Baltzer JL. 2015. CTFS-Forest GEO: A worldwide network monitoring forests in an era of global change. Global Change Biology 21: 528-549.

Anderson-Teixeira KJ, Wang MM, McGarvey JC, LeBauer DS. 2016. Carbon dynamics of mature and regrowth tropical forests derived from a pantropical database (T rop F or C-db). Global Change Biology 22: 1690-1709.

Baas P, Ewers FW, Davis SD, Wheeler EA. 2004. Evolution of xylem physiology. Hemsley AR, Poole I, editors. The evolution of plant physiology: from whole plants to ecosystems. London, UK: Elsevier, p273-295.

Baker TR, Coronado ENH, Phillips OL, Martin J, van der Heijden GM, Garcia M, Espejo JS. 2007. Low stocks of coarse woody debris in a southwest amazonian forest. Oecologia 152:495-504.

Boddy L. 2001. Fungal community ecology and wood decomposition processes in angiosperms: from standing tree to complete decay of coarse woody debris. Ecological Bulletins: 43-56.

Boddy L, Hynes J, Bebber DP, Fricker MD. 2009. Saprotrophic cord systems: dispersal mechanisms in space and time. Mycoscience 50: 9-19.

Boddy L, Owens EM, Chapela IH. 1989. Small scale variation in decay rate within logs one year after felling: Effect of fungal community structure and moisture content. FEMS Microbiology Letters 62: 173-183.

Bradford MA, Warren II RJ, Baldrian P, Crowther TW, Maynard DS, Oldfield EE, Wieder WR, Wood SA, King JR. 2014. Climate fails to predict wood decomposition at regional scales. Nature Climate Change 4: 625.

Brown S. 1997. Estimating biomass and biomass change of tropical forests: a primer. Rome, Italy: Food & Agriculture Org. 55p.

Carlson BS, Koerner SE, Medjibe VP, White LJ, Poulsen JR. 2017. Deadwood stocks increase with selective logging and large tree frequency in Gabon. Global Change Biology 23: 1648-1660.

Chambers JQ, Higuchi N, Schimel JP, Ferreira LV, Melack JM. 2000. Decomposition and carbon cycling of dead trees in tropical forests of the central Amazon. Oecologia 122: 380-388.

Chave J, Condit R, Lao S, Caspersen JP, Foster RB, Hubbell SP. 2003. Spatial and temporal variation of biomass in a tropical forest: results from a large census plot in Panama. Journal of Ecology 91: 240-252.

Christensen O. 1977. Estimation of standing crop and turnover of dead wood in a Danish oak forest. Oikos 28: 177-186.

Clark DA, Brown S, Kicklighter DW, Chambers JQ, Thomlinson JR, Ni J. 2001. Measuring net primary production in forests: concepts and field methods. Ecological Applications 11: 356-370.

Clark DB, Clark DA, Brown S, Oberbauer SF, Veldkamp E. 2002. Stocks and flows of coarse woody debris across a tropical rain forest nutrient and topography gradient. Forest Ecology and Management 164: 237-248.

Clay NA, Donoso DA, Kaspari M. 2015. Urine as an important source of sodium increases decomposition in an inland but not coastal tropical forest. Oecologia 177: 571-579.

Cleveland CC, Taylor P, Chadwick KD, Dahlin K, Doughty CE, Malhi Y, Smith WK, Sullivan BW, Wieder WR, Townsend AR. 2015. A comparison of plot-based satellite and Earth system

model estimates of tropical forest net primary production. Global Biogeochemical Cycles 29: 626-644.

Cornelissen JHC, Sass-Klaassen U, Poorter L, van Geffen K, van Logtestijn RSP, van Hal J, Goudzwaard L, Sterck FJ, Klaassen RKWM, Freschet GT, van der Wal A, Eshuis H, Zuo J, de Boer W, Lamers T, Weemstra M, Cretin V, Martin R, Ouden Jd, Berg MP, Aerts R, Mohren GMJ, Hefting MM. 2012. Controls on coarse wood decay in temperate tree species: birth of the LOGLIFE experiment. AMBIO 41: 231-245.

Cornwell WK, Cornelissen JHC, Allison SD, Bauhus J, Eggleton P, Preston CM, Scarff F, Weedon JT, Wirth C, Zanne AE. 2009. Plant traits and wood fates across the globe: rotted, burned, or consumed? Global Change Biology 15: 2431-2449.

Cushman KC, Muller-Landau HC, Condit RS, Hubbell SP. 2014. Improving estimates of biomass change in buttressed trees using tree taper models. Methods in Ecology and Evolution 5: 573-582.

Delaney M, Brown S, Lugo AE, Torres-Lezama A, Quintero NB. 1998. The quantity and turnover of dead wood in permanent forest plots in six life zones of Venezuela. Biotropica 30: 2-11.

Delignette-Muller ML, Dutang C. 2015. fitdistrplus: An R package for fitting distributions. Journal of Statistical Software 64: 1-34.

Doughty CE, Metcalfe DB, Girardin CAJ, Amézquita FF, Cabrera DG, Huasco WH, Silva-Espejo JE, Araujo-Murakami A, da Costa MC, Rocha W, Feldpausch TR, Mendoza ALM, da Costa ACL, Meir P, Phillips OL, Malhi Y. 2015. Drought impact on forest carbon dynamics and fluxes in Amazonia. Nature 519: 78.

Eaton JM, Lawrence D. 2006. Woody debris stocks and fluxes during succession in a dry tropical forest. Forest Ecology and Management 232: 46–55.

Falster DS, Duursma RA, Baltzer JL, Baraloto C, Battaglia M, Battles JJ, Bond-Lamberty B, van Breugel M, Camac J, Claveau Y. 2015. BAAD: a Biomass And Allometry Database for woody plants.

Fasth BG, Harmon ME, Sexton J, White P. 2011. Decomposition of fine woody debris in a deciduous forest in North Carolina. The Journal of the Torrey Botanical Society 138: 192-206.

Gora EM, Battaglia LL, Schumacher HB, Carson WP. 2014. Patterns of coarse woody debris volume among 18 late-successional and mature forest stands in Pennsylvania1. The Journal of the Torrey Botanical Society 141: 151-160.

Gurdak DJ, Aragão LE, Rozas-Dávila A, Huasco WH, Cabrera KG, Doughty CE, Farfan-Rios W, Silva-Espejo JE, Metcalfe DB, Silman MR. 2014. Assessing above-ground woody debris dynamics along a gradient of elevation in Amazonian cloud forests in Peru: balancing above-ground inputs and respiration outputs. Plant Ecology & Diversity 7: 143-160.

Harmon ME, Franklin JF, Swanson FJ, Sollins P, Gregory SV, Lattin JD, Anderson NH, Cline SP, Aumen NG, Sedell JR, Lienkaemper GW, Cromack K, Jr, Cummins KW. 1986. Ecology of coarse woody debris in temperate ecosystems. Advances in Ecological Research 15: 133-302.

Harmon ME, Sexton J. 1996. Guidelines for measurements of woody detritus in forest ecosystems. Publication Number 20, US LTER Network Office, University of Washington, Washington, USA, p73.

Harmon ME, Whigham DF, Sexton J, Olmsted I. 1995. Decomposition and mass of woody detritus in the dry tropical forests of the northeastern Yucatan Peninsula, Mexico. Biotropica: 305-316.

Hubbell SP, Foster RB. 1983. Diversity of canopy trees in a neotropical forest and implications for conservation. Sutton SL, Whitmore TC, Chadwick AC, editors. Tropical rain forest: ecology and management. Oxford: Blackwell Scientific, p25-41.

Iwashita DK, Litton CM, Giardina CP. 2013. Coarse woody debris carbon storage across a mean annual temperature gradient in tropical montane wet forest. Forest Ecology and Management 291: 336-343.

Janisch J, Harmon M. 2002. Successional changes in live and dead wood carbon stores: implications for net ecosystem productivity. Tree Physiology 22: 77-89.

Johnsson M, Stallard R. 1989. Physiographic controls on the composition of sediments derived from volcanic and sedimentary terrains on Barro Colorado Island, Panama. Journal of Sedimentary Research 59: 768-781.

Kaspari M, Yanoviak SP, Dudley R, Yuan M, Clay NA. 2009. Sodium shortage as a constraint on the carbon cycle in an inland tropical rainforest. Proceedings of the National Academy of Sciences 106: 19405-19409.

Keller M, Palace M, Asner GP, Pereira R, Silva JNM. 2004. Coarse woody debris in undisturbed and logged forests in the eastern Brazilian Amazon. Global Change Biology 10: 784-795.

Kissing LB, Powers JS. 2010. Coarse woody debris stocks as a function of forest type and stand age in Costa Rican tropical dry forest: long-lasting legacies of previous land use. Journal of Tropical Ecology 26: 467–71.

Král K, Janík D, Vrška T, Adam D, Hort L, Unar P, Šamonil P. 2010. Local variability of stand structural features in beech dominated natural forests of Central Europe: implications for sampling. Forest Ecology and Management 260: 2196-2203.

Lang GE, Knight DH. 1979. Decay rates for boles of tropical trees in Panama. Biotropica 11: 316-317.

Larjavaara M, Muller-Landau HC. 2010. Comparison of decay classification, knife test, and two penetrometers for estimating wood density of coarse woody debris. Canadian Journal of Forest Research 40: 2313-2321.

Larjavaara M, Muller-Landau HC. 2011. Cross-section mass: an improved basis for woody debris necromass inventory. Silva Fennica 45: 291-298.

Leigh EG, Jr. 1999. Tropical Forest Ecology: A View from Barro Colorado Island: Oxford University Press, Oxford, England, UK.

Liski J, Palosuo T, Peltoniemi M, Sievänen R. 2005. Carbon and decomposition model Yasso for forest soils. Ecological Modelling 189: 168-182.

Maass JM, Martínez-Yrízar A, Patiño C, Sarukhán J. 2002. Distribution and annual net accumulation of above-ground dead phytomass and its influence on throughfall quality in a Mexican tropical deciduous forest ecosystem. Journal of Tropical Ecology 18: 821-834.

Mäkinen H, Hynynen J, Siitonen J, Sievänen R. 2006. Predicting the decomposition of Scots pine, Norway spruce, and birch stems in Finland. Ecological Applications 16: 1865-1879.

Malhi Y, Aragao LEO, Metcalfe DB, Paiva R, Quesada CA, Almeida S, Anderson L, Brando P, Chambers JQ, Da Costa AC. 2009. Comprehensive assessment of carbon productivity, allocation and storage in three Amazonian forests. Global Change Biology 15: 1255-1274.

Malhi Y, Doughty C, Galbraith D. 2011. The allocation of ecosystem net primary productivity in tropical forests. Philosophical Transactions of the Royal Society: B 366: 3225-3245.

Malhi Y, Farfán Amézquita F, Doughty CE, Silva-Espejo JE, Girardin CA, Metcalfe DB, Aragão LE, Huaraca-Quispe LP, Alzamora-Taype I, Eguiluz-Mora L. 2014. The productivity, metabolism and carbon cycle of two lowland tropical forest plots in south-western Amazonia, Peru. Plant Ecology & Diversity 7: 85-105.

Marvin DC, Asner GP. 2016. Branchfall dominates annual carbon flux across lowland Amazonian forests. Environmental Research Letters 11: 094027.

Meakem V, Tepley AJ, Gonzalez-Akre EB, Herrmann V, Muller-Landau HC, Wright SJ, Hubbell SP, Condit R, Anderson-Teixeira KJ. 2017. Role of tree size in moist tropical forest carbon cycling and water deficit responses. New Phytologist.

Metcalfe D, Meir P, Aragão LEOC, da Costa A, Almeida S, Braga A, Gonçalves P, Athaydes J, Malhi Y, Williams M. 2008. Sample sizes for estimating key ecosystem characteristics in a tropical terra firme rainforest. Forest Ecology and Management 255: 558-566.

Oberle B, Covey KR, Dunham KM, Hernandez EJ, Walton ML, Young DF, Zanne AE. 2017. Dissecting the effects of diameter on wood decay emphasizes the importance of cross-stem conductivity in Fraxinus americana. Ecosystems: 1-13.

Odum HT. 1970. Summary: an emerging view of the ecological system at El Verde. Odum HT, Pigeon RF editors. A tropical rain forest. A study of irradiation and ecology at El Verde, Puerto Rico. Oak Ridge: U.S. Atomic Commission.

Ovington J, Madgwick H. 1959. Distribution of organic matter and plant nutrients in a plantation of Scots pine. Forest Science 5: 344-355.

Palace M, Keller M, Asner GP, Silva JNM, Passos C. 2007. Necromass in undisturbed and logged forests in the Brazilian Amazon. Forest Ecology and Management 238: 309-318.

Palace M, Keller M, Hurtt G, Frolking S. 2012. A review of above ground necromass in tropical forests. Sudarshana P, Nageswara-Rao M, Soneji JR, editors. Tropical forests. Rijeka, Croatia: Intech, p215–252.

Palace M, Keller M, Silva H. 2008. Necromass production: studies in undisturbed and logged Amazon forests. Ecological Applications 18: 873-884.

Pan Y, Birdsey RA, Fang J, Houghton R, Kauppi PE, Kurz WA, Phillips OL, Shvidenko A, Lewis SL, Canadell JG, Ciais P, Jackson RB, Pacala SW, McGuire AD, Piao S, Rautiainen A, Sitch S, Hayes D. 2011. A large and persistent carbon sink in the world's forests. Science 333: 988-993.

Paton S. 2017. Report of the Physical Monitoring Program of the Smithsonian Tropical Research Institute. http://biogeodb.stri.si.edu/physical_monitoring/research/barrocolorado.

Pfeifer M., Lefebvre V, Turner E, Cusack J, Khoo M, Chey VK, Peni M, Ewers RM. 2015. Deadwood biomass: An underestimated carbon stock in degraded tropical forests? Environmental Research Letters 10:044019.

Přívětivý T, Janík D, Unar P, Adam D, Král K, Vrška T. 2016. How do environmental conditions affect the deadwood decomposition of European beech (*Fagus sylvatica L.*)? Forest Ecology and Management 381: 177-187.

R Core Team. 2017. R: A language and environment for statistical computing. Vienna, Austria: Foundation for Statistical Computing.

Rice AH, Pyle EH, Saleska SR, Hutyra L, Palace M, Keller M, de Camargo PB, Portilho K, Marques DF, Wofsy SC. 2004. Carbon balance and vegetation dynamics in an old-growth amazonian forest. Ecological Applications 14: 55-71.

Schnitzer SA, Bongers F. 2011. Increasing liana abundance and biomass in tropical forests: emerging patterns and putative mechanisms. Ecology Letters 14: 397-406.

Sierra CA, del Valle JI, Orrego SA, Moreno FH, Harmon ME, Zapata M, Colorado GJ, Herrera MA, Lara W, Restrepo DE, Berrouet LM, Loaiza LM, Benjumea JF. 2007. Total carbon stocks in a tropical forest landscape of the Porce region, Colombia. Forest Ecology and Management 243: 299-309.

Song Z, Dunn C, Lü X-T, Qiao L, Pang J-P, Tang J-W. 2017. Coarse woody decay rates vary by physical position in tropical seasonal rainforests of SW China. Forest Ecology and Management 385: 206-213.

Swift M, Healey I, Hibberd J, Sykes J, Bampoe V, Nesbitt M. 1976. The decomposition of branch-wood in the canopy and floor of a mixed deciduous woodland. Oecologia 26: 139-149.

Thornton PE. 1998. Regional ecosystem simulation: combining surface-and satellite-based observations to study linkages between terrestrial energy and mass budgets. Missoula: University of Montana, p280.

van der Heijden GM, Schnitzer SA, Powers JS, Phillips OL. 2013. Liana impacts on carbon cycling, storage and sequestration in tropical forests. Biotropica 45: 682-692.

van der Heijden GMF, Powers JS, Schnitzer SA. 2015. Lianas reduce carbon accumulation and storage in tropical forests. Proceedings of the National Academy of Sciences 112: 13267-13271.

van der Wal A, Ottosson E, de Boer W. 2015. Neglected role of fungal community composition in explaining variation in wood decay rates. Ecology 96: 124-133.

van Geffen KG, Poorter L, Sass-Klaassen U, van Logtestijn RSP, Cornelissen JHC. 2010. The trait contribution to wood decomposition rates of 15 Neotropical tree species. Ecology 91: 3686-3697.

Warren W, Olsen P. 1964. A line intersect technique for assessing logging waste. Forest Science 10: 267-276.

Weedon JT, Cornwell WK, Cornelissen JH, Zanne AE, Wirth C, Coomes DA. 2009. Global meta-analysis of wood decomposition rates: a role for trait variation among tree species? Ecology Letters 12: 45-56.

Woldendorp G, Keenan RJ, Barry S, Spencer RD. 2004. Analysis of sampling methods for coarse woody debris. Forest Ecology and Management 198: 133-148.

Wolf PR, Dewitt BA. 2000. Elements of photogrammetry: with applications in GIS: McGraw-Hill New York.

Zanne AE, Oberle B, Dunham KM, Milo AM, Walton ML, Young DF. 2015. A deteriorating state of affairs: How endogenous and exogenous factors determine plant decay rates. Journal of Ecology 103: 1421-1431.

Table Legends

Table 1: Key characteristics of the field datasets analyzed here. Elevated WD denotes whether we recorded the proportion of downed WD that did not directly contact the forest floor. The diameter range is for the diameter at the intersection with the transect in the case of downed WD, the trunk diameter at 1.3 m height in the case of standing WD, and the largest diameter of the piece in the case of suspended WD. Figure 2 depicts the layout of the dynamics plots and an example of the long transects. Asterisks indicate that we recorded whether the downed WD was elevated or in direct contact with the soil and superscript "L" indicates that we recorded whether WD pieces were lianas.

Table 2: The sample size, mass, and volume (±95% CI) of downed WD inputs separated into branchfall and treefall. The total volume only includes WD for which the source (branchfall, treefall, trunk wood, and/or branch wood) could be determined. Estimates for 2015 and 2016 were based on inputs of CWD into the dynamics plots, with mass calculated using penetrometer measurements, whereas 2017 estimates were based on the volume of WD stocks characterized using long transects. These are the only datasets that separated branchfall and treefall inputs. Further details in Tables S5 and S6.

Table 3: Sampling effort required to estimate the volume of WD pools and fluxes to within 10% of the true mean with 95% confidence. We present values from the smallest sampling scale in cases where multiple scales were recorded. The coefficient of variation (CV, with 95% CI) is the standard deviation divided by the mean of total volume per sampling unit, in percent. Asterisks indicate estimates of trunk wood and branch wood as a subset of treefalls (i.e., excluding branchfalls).

Table 4. Estimates of downed and standing CWD residence time and decomposition constant (±CI) using a steady state model and by averaging decomposition constants from individual pieces of CWD, weighted by their mass or cross-sectional mass. Residence time is the inverse of

the decomposition constant, k, in all cases ($\frac{1}{k}$). These steady state model estimates either use measured values of CWD inputs (raw inputs) or iteratively corrected inputs to account for decomposition that occurred before inputs were measured (iteratively corrected inputs). The individualized estimates either assume that the pieces of CWD leaving the pool decomposed entirely (maximum decomposition) or only lost enough volume to fall below the minimum measurement threshold (minimum decomposition).

Table 1

Woody Debris Pool	Sampling method	Diameter Range	Sampling effort (per year)	Years sampled	Sampling design	Density estimate	Total WD Pieces
Standing WD	Dynamics plots	>20 cm	16 ha	2009, 2010-2016	100 plots of 40x40 m, subsampled every 10x10 m	Penetrometer	855
		2-20 cm	0.79 ha	2009, 2010-2016	100 plots of 5 m radius centered in the dynamics plots	Mean only	97
Suspended WD	Dynamics plots	>20 cm	2 ha	2015	200 plots of 10x10 m, in each corner of 50 dynamics plots	Mean only	22
		5-20 cm					234
Downed WD	Dynamics plot transects	>20 cm	16 km	2009, 2010-2016	400 perpendicular transects of 40 m, subsampled every 10 m	Penetrometer	1766
	Long transects	>20 cm	8 km	2010	16 transects of 500 m, subsampled every 20m	Penetrometer, Disk-sampling	137
			8.5 km	2014		Penetrometer	136
		2-20 cm	0.4 km	2010	400 transect sections of 1 m, one in every 20m of the 500 m transects	Disk-sampling	176
			0.45 km	2014	450 transect sections of 1 m, one in every 20m of the 500 m transects	Mean only	161
		>10 cm*,L	15 km	2017	16 transects of 500 m and 7 perpendicular transects of 1000 m, subsampled every 20 m	Mean only	561
		<10 cm*,L	0.75 km	2017	750 transect sections of 1 m, one in every 20 m of the 2017 long transects	Mean only	329
	Short transects	>10 cm*	3.3 km	2015	100 m transects haphazardly distributed across BCI	Penetrometer	177

Table 2

Inputs or Stocks	Year	Woody Debris Pool or Inputs	Total Volume (m^3 ha^{-1})	Total WD Pieces (N)	Treefall Pieces (N)	Branchfall WD (% of Total)		Branch Wood (% of Treefall)	
						Volume	Mass	Volume	Mass
Inputs	2015	>20cm	7.8 (3.8, 12.9)	57	40	**18 (5, 36)**	**22 (5, 46)**	**5 (1, 13)**	**5 (1, 11)**
	2016	>20cm	11.5 (4.4, 22.7)	62	52	**5 (2, 15)**	**6 (2, 17)**	**12 (4, 35)**	**16 (4, 41)**
	2015-2016	>20cm	9.6 (5.1, 16.0)	119	92	**10 (4, 22)**	**13 (4, 28)**	**10 (4, 20)**	**12 (5, 25)**
Stocks	2017	2-10cm	8.2 (6.0, 10.6)	236	25	**79 (70, 88)**	N/A	**96 (95, 98)**	N/A
		10-20cm	5.2 (4.2, 6.3)	303	145	**49 (45, 53)**	N/A	**29 (24, 34)**	N/A
		>20cm	31.0 (52.3, 87.6)	231	198	**4 (3, 6)**	N/A	**6 (4, 8)**	N/A
		>2cm	66.5 (43.4, 103.0)	770	368	**17 (11, 26)**	N/A	**7 (4, 13)**	N/A

6 **Table 3**

Estimate method (unit)	Component	Sampling unit	Total sampling effort	Year (s)	Flux, stock, or sub-pool	Coefficient of Variation (%)	Required sampling effort (km or ha)
Transects (km)	Downed CWD (>20 cm)	10 m	112 km	2009-10, 2012-16	Stocks	601 (468, 769)	139 (84, 227)
			80 km	2010, 2013-16	Inputs	1369 (554, 2308)	720 (118, 2047)
					Outputs	1683 (577, 3085)	1088 (128, 3658)
	Downed CWD (>10 cm)	20 m	15 km	2017	Stocks	693 (149, 1483)	370 (17, 1695)
					Suspended above soil	386 (255, 576)	115 (50, 256)
					In contact with soil	889 (157, 2231)	609 (19, 3836)
					Branchfall	334 (239, 472)	86 (44, 172)
					Treefall	777 (165, 1760)	465 (21, 2388)
					Liana wood	2020 (0, 7673)	3145 (0, 45379)
					Trunk wood*	831 (157, 2041)	532 (19, 3211)
					Branch wood*	631 (344, 1083)	307 (91, 904)
	Downed FWD (<10 cm)	1 m	0.75 km	2017	Stocks	228 (161, 322)	2 (1, 4)
					Branchfall	322 (228, 426)	4 (2, 7)
					Treefall	664 (360, 1258)	17 (5, 61)
					Liana wood	789 (360, 1720)	24 (5, 114)
					Trunk wood*	738 (395, 1468)	21 (6, 83)
					Branch wood*	1610 (0, 6490)	100 (0, 1625)
Plots (ha)	Standing CWD	100 m^2	112 ha	2009-10, 2012-16	Stocks	1210 (600, 1830)	560 (139, 1280)
			80 ha	2010, 2013-16	Inputs	1610 (840, 2670)	956 (282, 2564)
					Outputs	1580 (860, 2580)	661 (149, 2009)
	Standing FWD	78.5 m^2	0.785 ha	2010	Stocks	450 (80, 1560)	63 (2, 756)
	Suspended CWD	100 m^2	2 ha	2015	Stocks	410 (200, 890)	64 (16, 308)
	Suspended FWD					180 (120, 260)	12 (6, 26)

Table 4

CWD pool	Calculation approach	Estimate type	Residence time (years)	
			Mass	Volume
Downed CWD	Steady State Model	Iteratively corrected inputs divided by stocks	3.44 (2.56, 4.68)	3.58 (2.62, 5.02)
		Raw inputs divided by stocks	3.96 (2.93, 5.40)	4.10 (3.00, 5.57)
	Average of individual CWD pieces	Minimum decomposition	15.29 (13.19, 17.86)	N/A
		Maximum Decomposition	1.85 (1.69, 2.00)	N/A
Standing CWD	Steady State Model	Iteratively corrected inputs divided by stocks	1.84 (1.21, 2.89)	2.01 (1.36, 3.03)
		Raw inputs divided by stocks	2.38 (1.57, 3.85)	2.55 (1.63, 3.93)
	Average of individual CWD pieces	Minimum decomposition	29.24 (21.4, 42.28)	N/A
		Maximum Decomposition	3.87 (3.13, 4.85)	N/A

Figure Legends

Fig. 1. The major pools and fluxes of woody debris as it cycles from living woody tissues to carbon dioxide and/or soil organic matter. Within each pool (standing, suspended, and downed), WD is separated into coarse and fine woody debris to represent how it is recorded. Filled black arrows indicate fluxes in and out of dead WD pools, whereas unfilled white arrows represent fluxes among pools of dead woody debris. Arrows and boxes are not scaled to represent the magnitude of fluxes and pools.

Fig. 2. The layout of each dynamics plot (Panel A) and an example of the long transects surveys (Panel B). As for the 40x40m plot in Panel A, dashed lines represent transects for monitoring downed CWD. Diagonally hashed squares represent sub-plots for quantifying suspended WD volume (area = 100 m^2), whereas the circular cross-hashed area represents the sub-plot for recording standing FWD (area = 78.5 m^2). Standing CWD was recorded throughout the entire 40x40m plot (area = 1600 m^2). As for Panel B, the rectangle represents the 50 ha forest dynamics plot and the dashed lines depict transects from the 2010 long transects surveys. Surveys in 2014 were similar in orientation, but offset by 10m. The North-to-South transects in 2017 were also accompanied by transects running West-to-East.

Fig. 3. The pools and fluxes of woody debris mass estimated in this study. Boxes are scaled to represent the relative mass of stocks in each pool (total WD stocks: 20.63 Mg ha-1). The aggregate totals of the downed and standing CWD (>20 cm diameter) inputs and outputs for are depicted as filled arrows, but fluxes of FWD and suspended CWD are not shown here because they were not quantified in this study. The arrows are proportional to the estimated fluxes at the point where they enter and exit the CWD stocks; the rest of the arrows are merely scaled to the size of the relevant stock because these sub-fluxes were not separately quantified. Estimated downed and standing CWD mass are based on penetrometer estimates from the 40x40m plots, whereas the other estimates use average density and volume from the 2010 and 2014 long

transects (downed FWD) or subplots within the 40x40m plots (standing FWD and all suspended WD).

Fig. 4. Panel A shows the percent of volume (mean ±95% CI) in downed WD >10cm diameter that was elevated above the forest floor within the 50 ha plot (2017 long transects) and across the entire island (2015 short transects). Panel B depicts the percent of volume (mean ±95% CI) elevated above the forest floor within each decomposition class (higher numbers indicate more advanced decomposition) recorded along the 2015 short transects.

Fig. 5. Annual variability in estimated downed and standing WD stocks (A) and CWD inputs (B) as mass (Mg ha^{-1}) with 95% confidence intervals based on data from the 40x40m dynamics (filled symbols). Also presented are the estimated stocks from the long transects in 2010 and 2014 (open symbols). See Figure S2 for parallel estimates of WD volume.

47 Fig. 1

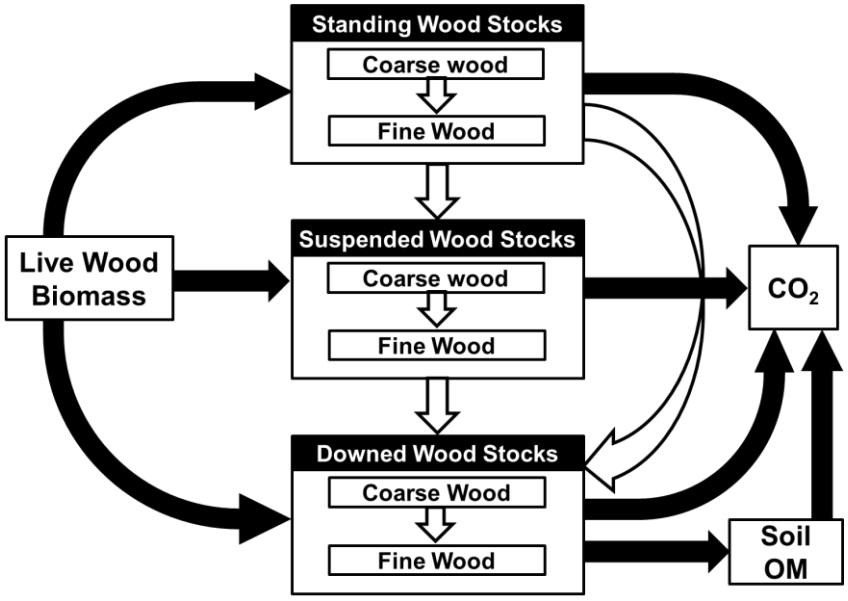
Standing Wood Stocks
Coarse wood
Fine Wood
Suspended Wood Stocks
Coarse wood
Fine Wood
Downed Wood Stocks
Coarse Wood
Fine Wood
Live Wood Biomass
CO_2
Soil OM

48

49

Fig. 2

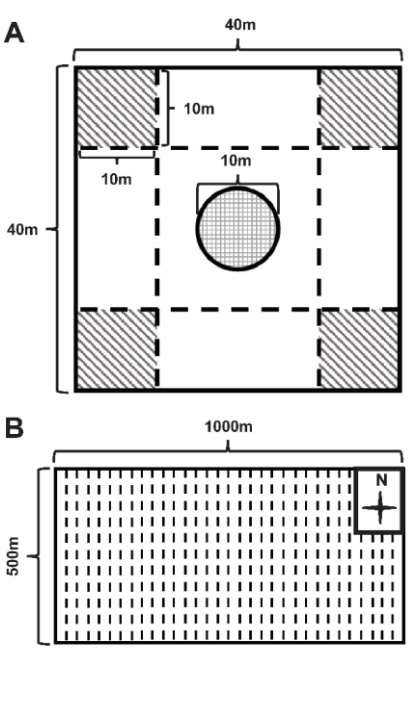

53 Fig. 3

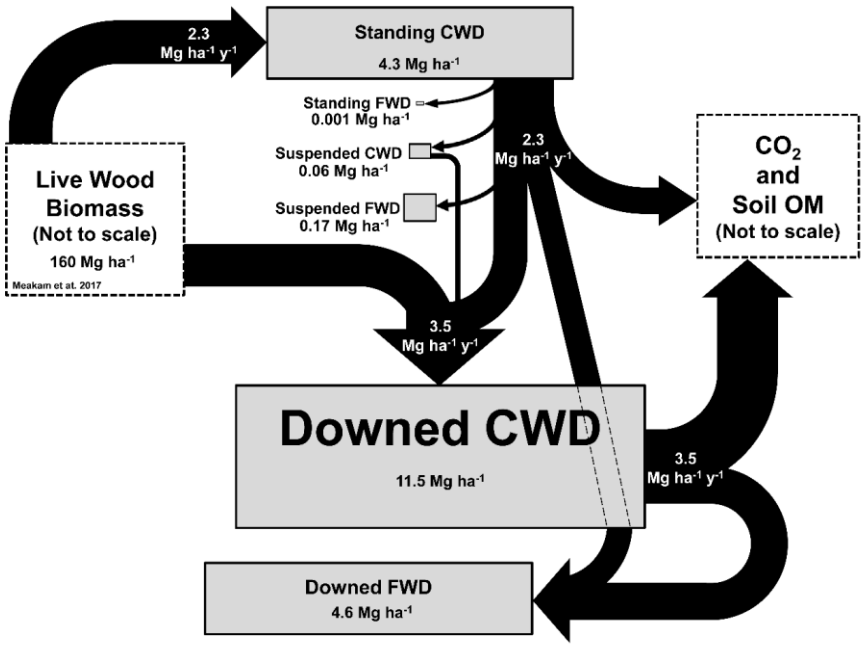
2.3
Mg ha-1 y-1
Standing CWD
4.3 Mg ha-1
Standing FWD
0.001 Mg ha-1
Suspended CWD
0.06 Mg ha-1
Suspended FWD
0.17 Mg ha-1
2.3
Mg ha-1 y-1
CO2
and
Soil OM
(Not to scale)
Live Wood
Biomass
(Not to scale)
160 Mg ha-1
Meakam et al. 2017
3.5
Mg ha-1 y-1
Downed CWD
11.5 Mg ha-1
3.5
Mg ha-1 y-1
Downed FWD
4.6 Mg ha-1

54

55

56 Fig. 4

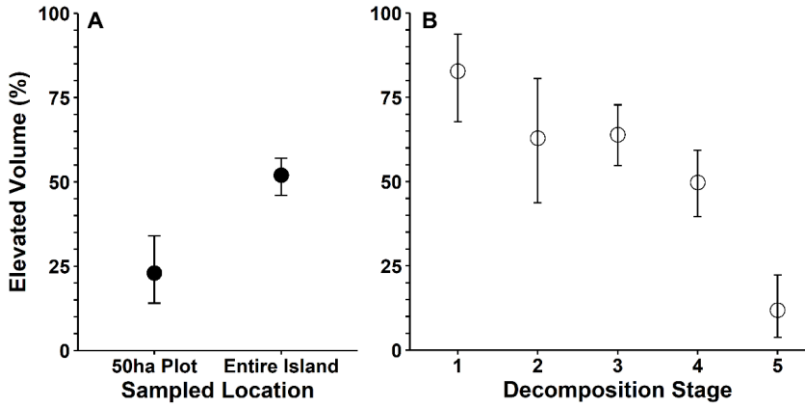

57

58

59

Fig. 5

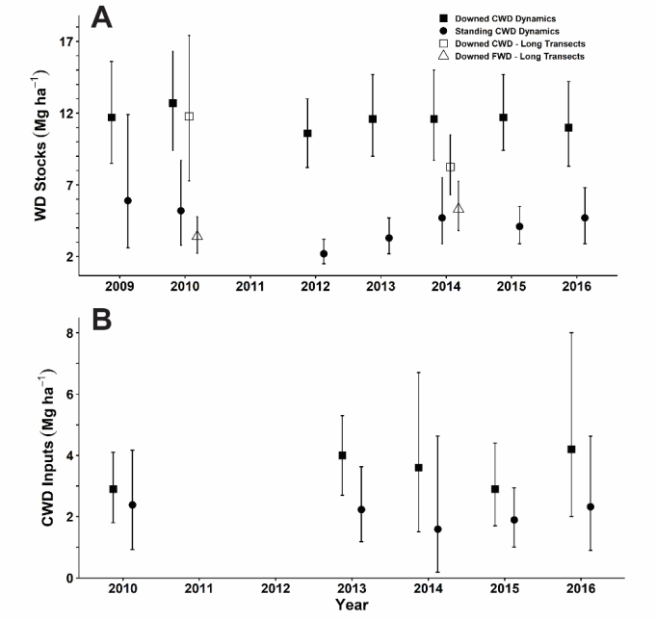
A
Downed CWD Dynamics
Standing CWD Dynamics
Downed CWD - Long Transects
Downed FWD - Long Transects
WD Stocks (Mg ha^{-1})
17
12
7
2
2009
2010
2011
2012
2013
2014
2015
2016
B
CWD Inputs (Mg ha^{-1})
8
6
4
2
0
2010
2011
2012
2013
2014
2015
2016
Year